Available online at www.sciencedirect.com
ScienceDirect
Journal of Solid State Chemistry 180 (2007) 1977–1983
JOURNAL OF SOLID STATE CHEMISTRY
www.elsevier.com/locate/jssc

Structural observations on $La_2(Ni,Co)O_{4\pm\delta}$ phases determined from *in situ* neutron powder diffraction

Stephen J. Skinner[a,*], Gisele Amow[b]

[a]*Department of Materials, Imperial College London, Prince Consort Road, London SW7 2BP, UK*
[b]*Air Vehicle Research Section (AVRS), Defence Research and Development Canada, National Defence Headquarters, Ottawa, ON, Canada K1A 0K2*

Received 8 March 2007; received in revised form 19 April 2007; accepted 30 April 2007
Available online 6 May 2007

Abstract

In situ neutron powder diffraction data have been analysed for a number of compositions in the solid solution series $La_2Ni_{1-x}Co_xO_{4\pm\delta}$ over the temperature range 150–650 °C. High-quality Rietveld refinements indicate no major structural transitions have occurred in any of the compositions, although close examination of the Ni/Co–O bond distances highlight changes in the coordination environment with increasing temperature. Further, the changes in the coordination can be correlated to changes in both the oxide ion and electronic conductivity indicating a direct link between transport properties, bonding and transition metal valence state in these Co containing layered perovskites.

Keywords: $La_2(Ni; Co)O_4$; Neutron diffraction; Bond lengths; Conductivity; Layered perovskites

1. Introduction

Ruddlesden-Popper phases ($A_{n+1}B_nO_{3n+1}$) have received considerable interest recently as potential cathode materials for solid oxide fuel cells. Much of the initial work on these phases has focused on the $Ln_2NiO_{4+\delta}$ ($n=1$) materials, where Ln = La, Pr, Nd, Sm, and has concentrated primarily on the electrochemical and transport properties of, in particular, the $La_2NiO_{4+\delta}$ composition. Several groups have investigated the un-substituted materials with Bassat et al. [1–3], Kharton et al. [4] and Skinner et al. [5] finding fast oxide ion conductivity over a wide range of temperatures indicating that there was potential for use as a cathode material. Further work focused on optimization of the parent composition either through A and/or B site substitution in an effort to maximize both the electronic and ionic conductivity of the materials. Standard substitutions such as Sr for La were performed and initial attempts have been made to investigate the substitution of Co for Ni on the B site [6–9] with transport properties determined through both isotopic exchange [10] and e.m.f. measurements [11–13]. Further recent work has investigated the performance of $Nd_2NiO_{4+\delta}$-based compositions in single fuel cells and in short cell stacks and reported encouraging results [14–18].

One of the most interesting features of the Co-doped $La_2NiO_{4\pm\delta}$ materials as potential cathodes has been the remarkably high low-temperature ionic conductivity (450–600 °C), as determined through isotopic exchange measurements of the oxide ion diffusion coefficient, coupled with changes in the activation energy of the diffusion coefficients [10]. This variation in the activation energy of diffusion could be associated with structural transformations on heating or with changes in the oxide ion diffusion mechanism, possibly as the stoichiometry varies from hyper-stoichiometry to hypo-stoichiometry. If there were a change in the mechanism it is likely that it would be associated with a change from an interstitialcy to vacancy conduction mechanism. Of course, there have been numerous studies of the crystal structure of K_2NiF_4 type oxides that have identified slight structural distortions depending on temperature and composition, with both tetragonal and orthorhombic models identified [19–27].

*Corresponding author. Fax: +44 20 7594 6757.
E-mail address: s.skinner@imperial.ac.uk (S.J. Skinner).

0022-4596/$ - see front matter Crown Copyright © 2007 Published by Elsevier Inc. All rights reserved.
doi:10.1016/j.jssc.2007.04.020

However, the majority of studies have concentrated on low temperature structural investigations with only a few studies [28,29] considering the *in situ* characterization of these types of oxides.

From the studies of the transport properties it was evident that there was great potential to exploit these materials, however many questions remained over their high temperature stability and structural transformations. In this contribution *in situ* high-temperature neutron powder diffraction data has been collected for three members of the $La_2Ni_{1-x}Co_xO_{4\pm\delta}$ solid solution series and the structural data obtained interpreted with reference to earlier work on both the oxide ion diffusion and electronic conductivity of these materials.

2. Experimental

Materials of composition $La_2Ni_{1-x}Co_xO_{4\pm\delta}$ ($x = 0.5$, 0.8, 1.0) were prepared by a modified Pechini type synthesis starting with solutions of the appropriate nitrates as described elsewhere [8,30]. After completion of the synthesis each material was examined by powder X-ray diffraction using a Bruker D8 diffractometer with CuK_α radiation and each composition was confirmed as being single phase and of the K_2NiF_4 structure type. Oxygen stoichiometry of the as-prepared materials was determined by iodometric titration and has been reported previously [10]. The room temperature oxygen hyper-stoichiometry for these materials was determined as $La_2CoO_{4.147(6)}$, $La_2Ni_{0.2}Co_{0.8}O_{4.113(3)}$ and $La_2Ni_{0.5}Co_{0.5}O_{4.147(4)}$ for the three materials under consideration at room temperature [10].

Cation stoichiometry for these materials was confirmed through Inductively Coupled Plasma Mass Spectrometry (ICP-MS). Behaviour of the materials on heating under air was determined from combined thermogravimetric and differential scanning calorimetry measurements (Netzsch Jupiter STA449C) with alumina sample holders and a heating rate of 20 °C min^{-1}. Neutron diffraction data were collected from the high-resolution powder diffractometer (HRPD) at the ISIS spallation source, Rutherford Appleton Laboratories, UK, over the temperature range of 150–650 °C. Each sample was contained in a quartz ampoule under a static $O_{2(g)}$ pressure of 200 mbar to mimic the conditions used in the previous isotopic exchange measurements. All data were analysed using the GSAS data refinement package [31] with lattice parameters and bond lengths extracted. Fractional occupancies of the B cation sites were set to the values obtained by ICP-MS analysis for the nickel–cobalt substituted materials.

3. Results and discussion

Three possible models were identified for the structural analysis of these materials: one tetragonal (space group *I*4/*mmm*) and two orthorhombic (space groups *Bmab* and *Fmmm*). It is well documented that the $La_2CoO_{4\pm\delta}$ composition adopts *Bmab* symmetry [32–34] at room temperature whereas the $La_2NiO_{4\pm\delta}$ material has been shown to adopt all three symmetries depending on synthesis conditions, oxygen stoichiometry and temperature [19,22–27,29,35–39]. Preliminary studies of the structure of the solid solution series under ambient conditions [8,40] indicated that the higher Co content materials (>60% Co) would adopt the *Bmab* symmetry with the lower Co content materials adopting orthorhombic *Fmmm* or tetragonal symmetry. Hence all of the compositions investigated here were analysed in *Bmab*, *Fmmm* and *I*4/*mmm* symmetries at all temperatures. Attempts to include discrete oxygen interstitial positions corresponding to excess oxygen in these refinements were unsuccessful. It may, of course, be a feature of these materials that at elevated temperatures the oxide ion positions are highly mobile, as discussed by Munnings et al. [10], and thus defining discrete oxygen interstitial positions becomes extremely difficult. Indeed from the electron density maps generated from the neutron powder diffraction data there was no evidence for oxygen interstitial content at elevated temperatures, and in some cases there was the possibility of a small degree of oxygen deficiency. Whilst this would seem unlikely, giving rise to Co^+, there have been previous reports of a $La_2CoO_{3.86}$ composition [34,41]. There is also support for the reduction of the $Co^{2+/3+}$ species from the TGA data, Fig. 1, in which a clear overall weight loss of 2.05% is observed for the $x = 1.0$ composition. This would correspond with a reduction to a hypo-stoichiometric phase. Evidently any oxygen contents determined solely from the refinements would therefore be subject to some uncertainty and are thus not considered further in this discussion.

Consideration of the goodness-of-fit parameters and the overall fit determined which of the proposed structural models would be adopted. It was clear that for all compositions at lower temperatures there was significant peak broadening that sharpened markedly on heating as illustrated for the $x = 0.5$ and 1.0 compositions in Fig. 2. This could be a result of the fine powder size and morphology obtained from the solution processing route, but could also indicate that more than one discrete phase

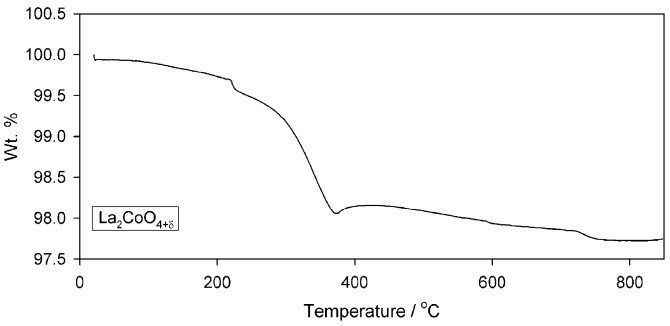

Fig. 1. Thermogravimetric analysis of a $La_2CoO_{4+\delta}$ sample on heating in flowing air highlighting significant weight loss at temperatures above ~200 °C.

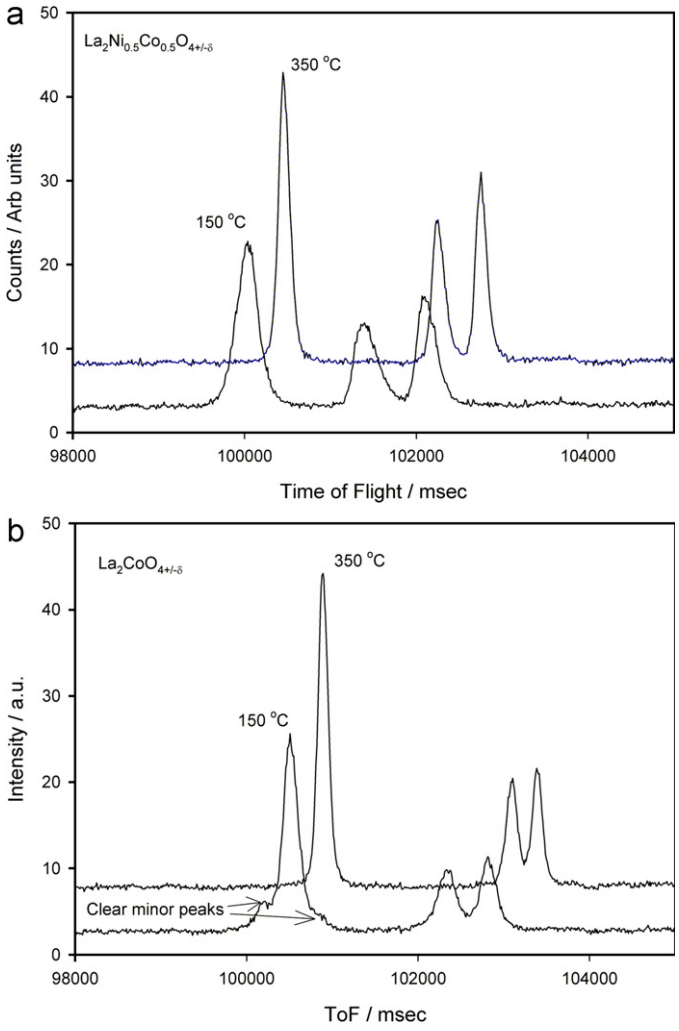

Fig. 2. Powder neutron diffraction data obtained from the (a) $La_2Ni_{0.5}Co_{0.5}O_{4\pm\delta}$ sample and (b) $La_2CoO_{4\pm\delta}$ sample at 150 and 350 °C on heating in air, highlighting the broadening at lower temperatures and the minority second phase in $La_2CoO_{4\pm\delta}$ material at low temperatures. (Data recorded at 350 °C has been offset on the *y*-axis in each case.)

was present, perhaps with differing oxygen stoichiometries. A further possibility would, of course, be the presence of strain within the materials. Despite this minor uncertainty all patterns fitted well and lattice parameters could be extracted with good statistics. The goodness-of-fit parameters for all refinements are given in Table 1 along with the space group attribution for each refinement. In each refinement where different models were proposed the refined parameters were applied in the same order and to the same degree, i.e., the refinements were identical for each model. Only the refinements with the lowest R_p, R_{wp} and χ^2 values were adopted as being correct. A typical refined powder pattern is shown for the $La_2CoO_{4\pm\delta}$ sample recorded at 650 °C in air in Fig. 3 with all atomic positions shown in Table 2, highlighting the excellent fit to the tetragonal model.

Initial observations of the powder diffraction patterns obtained indicated no clear peak splitting in the data collected at lower temperatures and no clear phase attribution or phase transformation could be discerned until full refinements of the data had been performed. From these refinements it was clear that the structure of all three compositions ($x = 0.5$, 0.8 and 1.0) at lower temperatures adopts the orthorhombic *Bmab* structure and that on heating in air there is a gradual reduction of the orthorhombic distortion until, in the case of the $x = 0.5$ material, the tetragonal polymorph is adopted at temperatures above 350 °C, Fig. 4(a) and Table 1. In the $x = 0.8$ and 1.0 samples the transformation to the tetragonal polymorph occurs at a slightly lower temperature of between 150 and 350 °C, Figs. 4(b) and (c). These changes are also reflected in the expansion of the *c*-parameter with a deviation from linearity occurring at approximately 350 °C with clear linear behaviour at higher temperatures, Fig. 5. In addition, the $x = 1.0$ material is, at low temperatures, a biphasic mixture of two discrete orthorhombic phases, both of *Bmab* symmetry, as there are key areas in the powder pattern where the peaks split on increasing the a/b distortion as is seen in Fig. 6.

The first phase of the $x = 1.0$ biphasic mixture has been refined with lattice parameters of $a = 5.4861(3)$, $b = 5.5320(4)$, and $c = 12.6982(7)$ Å constituting 32% of the sample by weight with the second phase having lattice parameters of $a = 5.51002(9)$, $b = 5.50425(9)$ and $c = 12.7165(1)$ Å constituting 68% by weight of the sample. On heating further these two phases interact until, as is evident from Fig. 2(b), only one discrete phase remains.

At this stage there is no clear difference in the structural chemistry among the three compositions investigated that could explain the differences observed in the characterization of the diffusion behaviour of the materials [10]. In order to further understand the structural characteristics of these compositions the variation of the bond lengths as a function of temperature for each composition was investigated. From Fig. 7 it is clear that the Ni/Co–O equatorial and apical bond distances vary significantly with composition. The Ni/Co–O bond lengths observed in all samples represent a distorted octahedral coordination environment around the B site as is typically found in A_2BO_4 oxides, with the equatorial and apical bond distances varying significantly with both composition and temperature. In Fig. 7(a) it is clear that the Ni/Co–O equatorial bonds for all compositions follow a linear expansion with increased temperature, as would be expected from the expansion of the *a* lattice parameter with the four equatorial metal–oxygen bonds being the key determinant in the a/b lattice parameter in the K_2NiF_4 type oxides. The main difference in these compositions arises in the apical Ni/Co–O bond lengths, Fig. 7(b). Clearly the variation of the apical bond lengths is non-linear and the behaviour between materials of different compositions also varies, with the $x = 0.5$ sample showing no variation of the bond length on heating from 500 to 550 °C (2.189(2) c.f. 2.188(2) Å) before a further increase in the bond length is observed on heating to 650 °C. For the $x = 0.8$ composition a local minimum in the apical bond length was found at 600 °C whilst for the

Table 1
Goodness-of-fit parameters and space group attribution for all refinements in the $La_2Ni_{1-x}Co_xO_{4\pm\delta}$ system

T/°C	$x = 1.0$				$x = 0.8$				$x = 0.5$			
	R_{WP} (%)	R_P (%)	χ^2	Space group	R_{WP} (%)	R_P (%)	χ^2	Space group	R_{WP} (%)	R_P (%)	χ^2	Space group
150	6.67	6.41	1.668	*Bmab*	6.70	5.70	1.640	*Bmab*	6.36	5.45	2.034	*Bmab*
350	5.77	4.86	1.295	*I4/mmm*	5.93	5.06	1.320	*I4/mmm*	5.61	4.77	1.570	*Bmab*
500	5.69	4.79	1.265	*I4/mmm*	5.74	4.83	1.251	*I4/mmm*	5.39	4.34	1.427	*I4/mmm*
550	5.68	4.8	1.269	*I4/mmm*	5.59	4.67	1.233	*I4/mmm*	5.31	4.50	1.391	*I4/mmm*
600	5.75	4.8	1.241	*I4/mmm*	5.59	4.68	1.228	*I4/mmm*	5.33	4.53	1.405	*I4/mmm*
650	5.99	5.02	1.184	*I4/mmm*	7.07	5.01	1.144	*I4/mmm*	5.38	4.58	1.391	*I4/mmm*

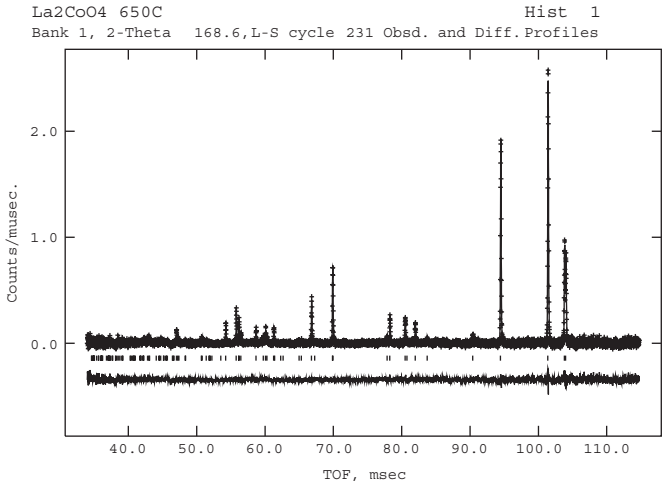

Fig. 3. Neutron ToF data recorded from $La_2CoO_{4\pm\delta}$ in a quartz ampoule *in situ* at 650 °C in 200 mbar O_2, $a = 3.91365(2)$ Å $c = 12.90156(8)$ Å, $R_p = 5.02\%$, $R_{wp} = 5.99\%$, $\chi^2 = 1.184$. Crosses are experimental data, solid line is the fit. Difference plot is displayed below the data and peak markers.

Table 2
Atomic positions and thermal parameters determined from La_2CoO_4 *in situ* at 650 °C in 200 mbar O_2 $R_p = 5.02\%$, $R_{wp} = 5.99\%$, $\chi^2 = 1.184$

Name	x	y	z	Ui/Ue*100	Fractn
LA1	0	0	0.36051(12)	2.86*	1
CO2	0	0	0	2.93*	0.991(15)
O3	0	0	0.17410(22)	7.97*	0.994(8)
O4	0	0.5	0	4.39*	0.983(9)

Thermal parameters multiplied by 100

Name	U11	U22	U33	U12	U13	U23
LA1	3.25(7)	3.25(7)	2.07(9)	0	0	0
CO2	2.31(25)	2.31(25)	4.2(5)	0	0	0
O3	9.79(15)	9.79(15)	4.33(24)	0	0	0
O4	3.14(16)	2.65(15)	7.38(23)	0	0	0

*Indicates thermal parameters were refined anisotropically and the values are given in the table below.

$x = 1.0$ sample a local maximum was observed at 550 °C, after which the bond distances for both samples converged to a common value of 2.24 Å at 650 °C. These transitions

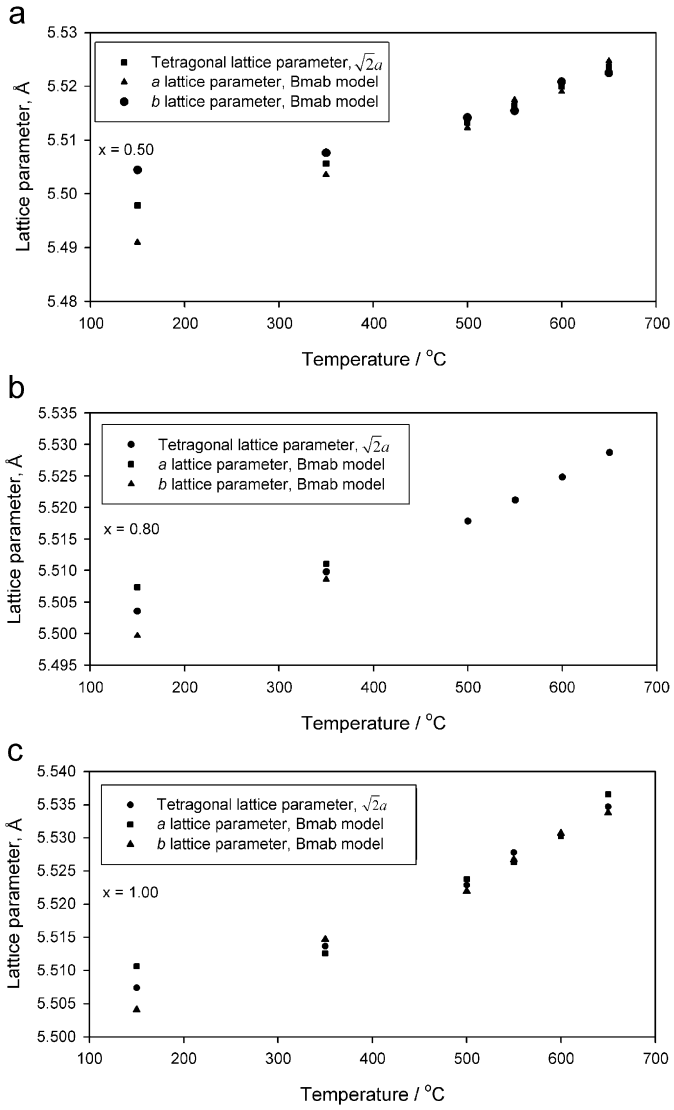

Fig. 4. Calculated lattice parameters for the $La_2Ni_{1-x}Co_xO_{4\pm\delta}$ system in both *I4/mmm* and *Bmab* space groups: (a) $x = 0.5$, (b) $x = 0.8$, and (c) $x = 1.0$ highlighting the convergence of the orthorhombic a and b parameters.

correlate with the temperatures at which changes in the diffusion behaviour were observed [10]. The Ni/Co–O distances for the equatorial bonds of all compositions are consistent with those reported by other authors such as

Von Lehmann [42] with 1.9439 Å, however, the apical bonds in the current work are significantly longer than the 2.0331 Å reported. In this current work we report minimum apical bond distances of 2.13 Å increasing to 2.26 Å on heating. The shorter 2.0331 Å apical bond distance reported by Von Lehmann would be more akin to a Co^{2+}(LS)–O bond distance.

The electronic structure of Co-containing materials is the subject of disagreement in the literature, with debate surrounding the nature of the ionic/covalent character of Co–O bonds. Takahashi et al. [43] have described the ostensibly Co^{3+} material, $LaCoO_3$ as having a significant degree of covalency and that spin state transitions, which occur within the material are a result of bond length variations with temperature and that the conductivity of $LaCoO_3$, including a metal–insulator transition, result from charge-transfer transitions rather than a Mott-Hubbard type transition. Further, Byeon and Demazeau [44] discuss the influence of LS–HS transitions in the K_2NiF_4 type oxides and consider the effect of the perovskite plane bonds (a/b) and c direction bonds on

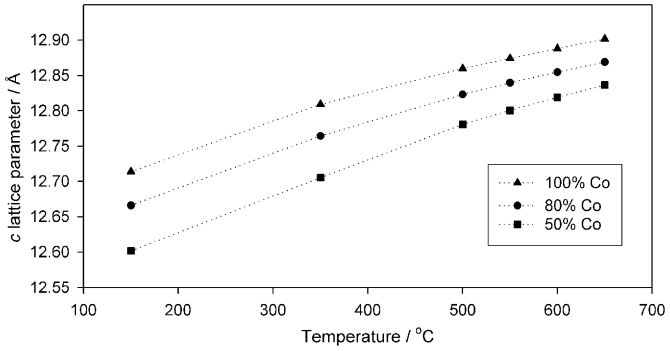

Fig. 5. Variation of c lattice parameter of $La_2Ni_{1-x}Co_xO_{4\pm\delta}$ ($x = 0.5$, 0.8 and 1.0) on heating in air.

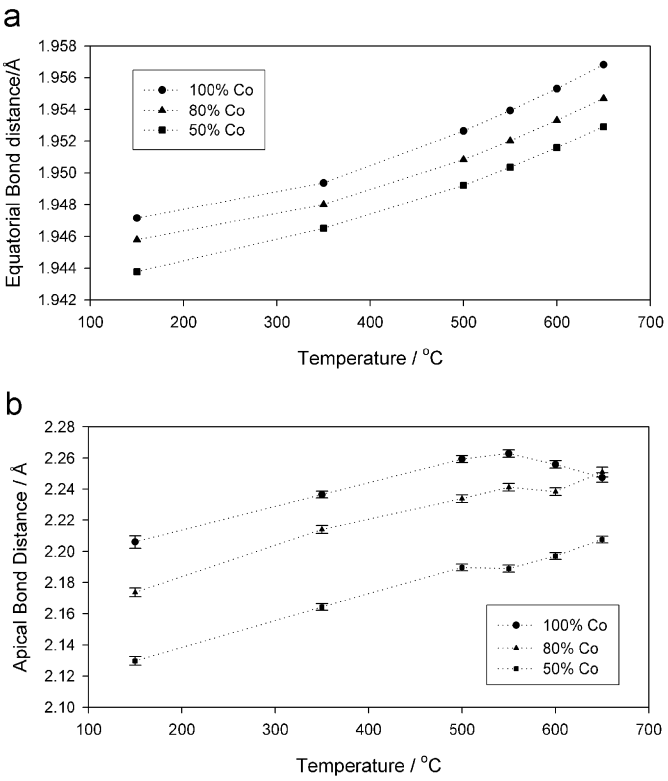

Fig. 7. Temperature dependence of the (a) equatorial and (b) apical Ni(Co)–O bond distances for the $La_2Ni_{1-x}Co_xO_{4\pm\delta}$ system.

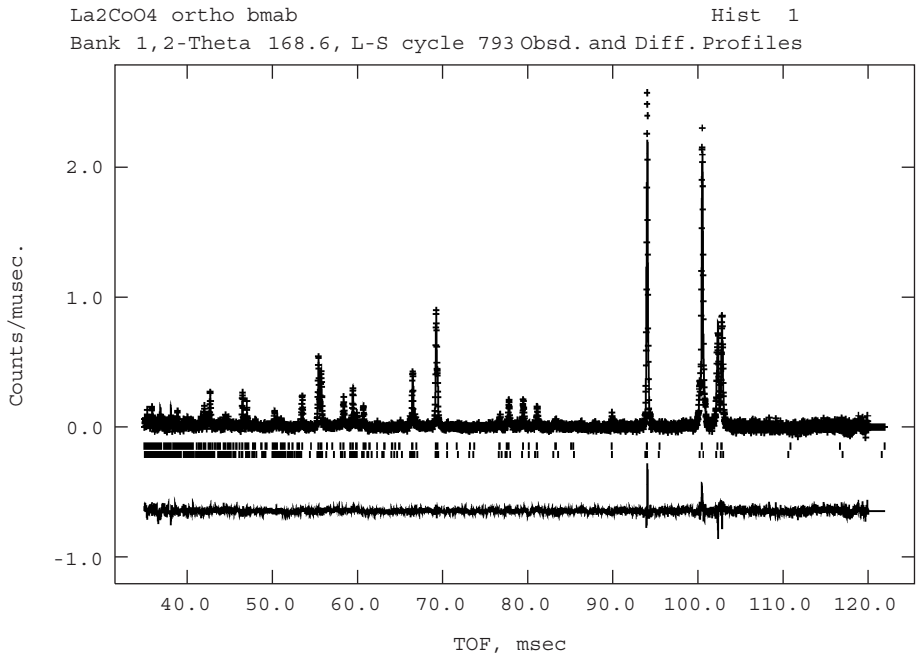

Fig. 6. Two phase fit of the neutron diffraction data for $La_2CoO_{4\pm\delta}$ recorded at 150 °C, $R_p = 6.41\%$, $R_{wp} = 6.67$, $\chi^2 = 1.668$. Crosses are experimental data, solid line is the fit. Difference plot is displayed below the data and peak markers. Inset highlights peak splitting.

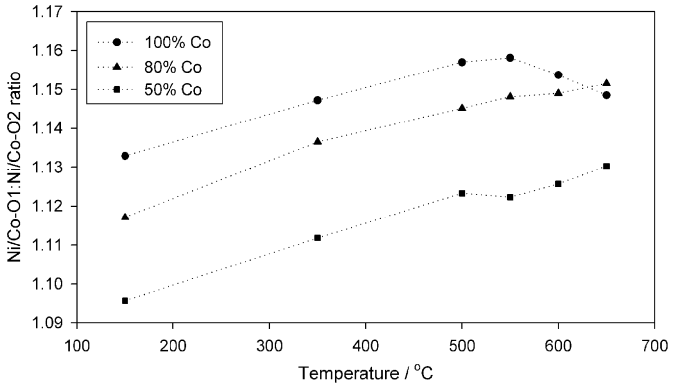

Fig. 8. Apical:Equatorial bond length ratio for the $La_2Ni_{1-x}Co_xO_{4\pm\delta}$ compositions where $x = 0.5$, 0.8 and 1.0.

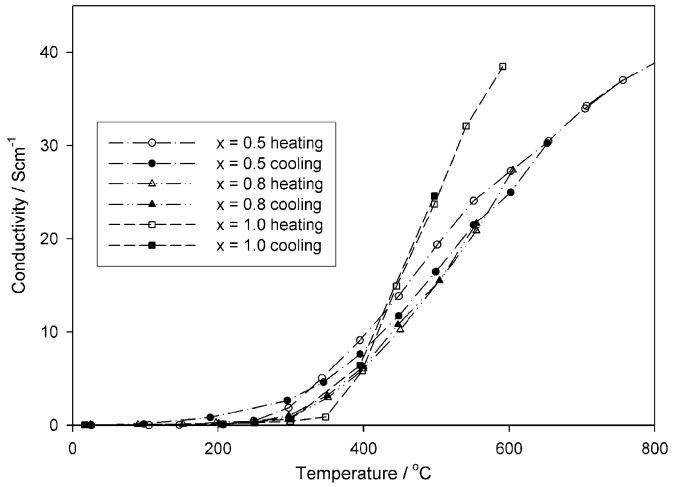

Fig. 9. Four point DC electrical conductivity data recorded on heating and cooling from the $La_2Ni_{1-x}Co_xO_{4\pm\delta}$ samples where $x = 0.5$, 0.8 and 1.0 indicating insulator–metal transition.

the covalency of the Co–O bonds. Hence it is feasible that there is some change in the degree of ionicity/covalency in the $La_2Ni_{1-x}Co_xO_4$ materials associated with variations in the transition metal spin state and hence conductivity. To further complicate the situation it has been reported that Co^{3+} at ambient temperature will adopt an intermediate spin state (IS) [45], resulting in bond distances intermediate between the expected HS and LS bond distances. Considering these features, in the materials discussed here it is therefore likely that there is a region of transition at approximately 550 °C where a number of factors influence the diffusion behaviour. From our observations it seems plausible that the electronic structure is affected by the change in the bond distances and that this may be related to a change in oxygen stoichiometry. If so, a slight reduction in the oxygen stoichiometry would also reduce the Co^{3+} ions leaving a predominantly $(Co/Ni)^{2+}$ environment. Hence at elevated temperatures a distorted environment resulting from the $3d^7$ Co^{2+} predominates. In the $x = 1.0$ sample the distorted environment, Fig. 8, peaks at 550 °C indicating a change in the nature of the bonding, suggesting that there is no longer predominantly $3d^7$ species present. Indeed given the reduction in the distortion it is conceivable that a reduced oxidation state is present, as suggested by some of the diffraction data. To further clarify these postulations it is intended to undertake X-ray absorption spectroscopy measurements to attempt to clarify the valence states of the transition metal cations present.

It is also of interest to note that these changes are coincident with a transition in the electrical conduction behaviour, from insulator to metal, as observed by Amow et al. [8], Fig. 9. In this earlier work it was noted that at a composition of 70% Co ($x = 0.70$) there is an increase in the total conductivity and this was attributed to the variation in the Co(Ni)–O–Co(Ni) bond distances. Indeed, it is likely that on increasing temperature the electronic state of the Co ions will change as has been intimated by Takahashi [43], in that spin state (as a result of oxygen content variances) and bond distance will change with temperature. Clearly bond distances and electronic behaviour are linked in these materials.

4. Conclusions

A series of samples of composition $La_2Ni_{1-x}Co_xO_{4\pm\delta}$ where $x = 0.5$, 0.8 and 1.0 have been characterized. Potential relationships between crystal structure, bonding, conductivity and electronic structure are discussed. From this it is clear that the behaviour of these materials at elevated temperatures is complex. Initial observations indicate that all of the orthorhombic structured materials transform to a simpler tetragonal form on heating, below the temperature at which changes in oxygen diffusion characteristics were previously observed. Investigation of the nature of the transition metal bonding highlights the distortion in the coordination environment due to the presence of $3d^7$ Co^{2+}. This distortion was found to vary significantly with Ni content and achieved a peak distortion at the relatively low temperature of 550 °C in the $x = 1.0$ sample. It is clear from these data that the changes in conductivity and coordination environment mirror changes in the diffusion behaviour reported previously and hence the changes in behaviour can be correlated.

Acknowledgments

The authors would like to thank the British Council and National Research Council Canada for funding this work through the Joint Science and Technology Committee. Thanks are also due to the CCLRC, UK, for providing access to the neutron powder diffraction facility, ISIS, at the Rutherford Appleton Laboratories. We are indebted to Dr. Geoff Fowler, Department of Civil Engineering, Imperial College London for access to the ICP-MS facility.

References

[1] J. M. Bassat, E. Boehm, J. C. Grenier, F. Mauvy, P. Dordor, M. Pouchard, in: J. Huijsmans (Ed.), Proceedings of the Fifth European Solid Oxide Fuel Cell Forum, Luzern, Switzerland, 2002, p. 586.

[2] E. Boehm, J. M. Bassat, F. Mauvy, P. Dordor, J. C. Grenier, M. Pouchard, in: A.J. McEvoy (Ed.), Proceedings of the 4th European Solid Oxide Fuel Cell Forum, Lucerne, Switzerland, 2000, p. 717.

[3] J.M. Bassat, P. Odier, A. Villesuzanne, C. Marin, M. Pouchard, Solid State Ionics 167 (2004) 341.

[4] V.V. Kharton, A.P. Viskup, E.N. Naumovich, F.M.B. Marques, J. Mater. Chem. 9 (1999) 2623.

[5] S.J. Skinner, J.A. Kilner, Solid State Ionics 135 (2000) 709.

[6] J.A. Kilner, C.K.M. Shaw, Solid State Ionics 154–155 (2002) 523.

[7] C.K.M. Shaw, Ph.D. Thesis, University of London, London, 2001.

[8] G. Amow, P. Whitfield, I. Davidson, R.P. Hammond, C. Munnings, S.J. Skinner, Solid State Inorganic Materials IV, Proceedings of the MRS, vol. 755, Boston, 2003, pp. 347–352.

[9] C.N. Munnings, S.J. Skinner, G. Amow, P. Whitfield, I. Davidson, Mixed ionic electronic conducting perovskites for advanced energy systems, in: N. Orlovskaya, N. Browning (Eds.), Proceedings of the NATO ARW on Mixed Ionic Electronic Conducting (MIEC) Perovskites for Advanced Energy Systems, Kyiv, Ukraine, 8–12 June 2003, Kluwer Academic Publishers, Drodrecht, July 2004, pp. 289–293.

[10] C.N. Munnings, S.J. Skinner, G. Amow, P.S. Whitfield, I.J. Davidson, Solid State Ionics 176 (2005) 1895.

[11] V.V. Kharton, A.P. Viskup, A.V. Kovalevsky, E.N. Naumovich, F.M.B. Marques, Solid State Ionics 143 (2001) 337.

[12] V.V. Kharton, A.A. Yaremchenko, A.L. Shaula, M.V. Patrakeev, E.N. Naumovich, D.I. Logvinovich, J.R. Frade, F.M.B. Marques, J. Solid State Chem. 177 (2004) 26.

[13] A.A. Yaremchenko, V.V. Kharton, M.V. Patrakeev, J.R. Frade, J. Mater. Chem. 13 (2003) 1136.

[14] F. Mauvy, C. Lalanne, J.M. Bassat, J.C. Grenier, H. Zhao, P. Dordor, P. Stevens, J. Eur. Ceram. Soc. 25 (2005) 2669.

[15] E. Boehm, J.M. Bassat, P. Dordor, F. Mauvy, J.C. Grenier, P. Stevens, Solid State Ionics 176 (2005) 2717.

[16] F. Mauvy, C. Lalanne, J.M. Bassat, J.C. Grenier, H. Zhao, L.H. Huo, P. Stevens, J. Electrochem. Soc. 153 (2006) A1547.

[17] F. Mauvy, J.M. Bassat, E. Boehm, J.P. Manaud, P. Dordor, J.C. Grenier, Solid State Ionics 158 (2003) 17.

[18] C. Lalanne, F. Mauvy, J.M. Bassat, J.C. Grenier, P. Stevens, G. Prosperi, J.V. herle, S. Diethelm, R. Ihringer, in: Seventh European Solid Oxide Fuel Cell Forum, Lucerne, Switzerland, 2006.

[19] J. Rodriguez-Caravajal, M.T. Fernandez-Diaz, J.L. Martinez, J. Phys.: Condens. Matter 3 (1991) 3215.

[20] R. Genouel, C. Michel, B. Raveau, Chem. Mater. 7 (1995) 2181.

[21] J.E. Lorenzo, J.M. Tranquada, D.J. Buttrey, V. Sachan, Phys. Rev. B 51 (1995) 3176.

[22] J. Jorgensen, B. Dabrowski, S. Pei, D. Richards, D. Hinks, Phys. Rev. B 40 (1989) 2187.

[23] Z. Hiroi, T. Obata, M. Takano, Y. Bando, Y. Takeda, O. Yamamoto, Phys. Rev. B 41 (1990) 11665.

[24] W. Paulus, A. Cousson, G. Heger, A. Revcolevschi, G. Dhalenne, S. Hosoya, Physica B 234–236 (1997) 20.

[25] H. Tamura, A. Hayashi, Y. Ueda, Physica C 258 (1996) 61.

[26] A. Mehta, P.J. Heaney, Phys. Rev. B 49 (1994) 563.

[27] H. Tamura, A. Hayashi, Y. Ueda, Physica C 216 (1993) 83.

[28] S.J. Skinner, Solid State Sci. 5 (2003) 419.

[29] W. Paulus, A. Cousson, G. Dhalenne, J. Berthon, A. Revcolevschi, S. Hosoya, W. Treutmann, G. Heger, R.L. Toquin, Solid State Sci. 4 (2002) 565.

[30] M. P. Pechini, US Patent No. 3,330,697 1967, 1967.

[31] R. B. Von Dreele, A.C. Larson, Los Alamos National Laboratory, 2001.

[32] R.M. Ram, P. Ganguly, C. Rao, Mater. Res. Bull. 23 (1988) 501.

[33] P. Lehude, M. Daire, C. R. Acad. Sci. Paris C 276 (1973) 1783.

[34] T. Kajitani, S. Hosoya, K. Hiraga, T. Fukuda, J. Phys. Soc. Jpn. 59 (1990) 562.

[35] I. Yazdi, S. Bhavaraju, J.F. DiCarlo, D.P. Scarfe, A.J. Jacobson, Chem. Mater. 6 (1994) 2078.

[36] I.D. Brown, Z. Kristallogr. 199 (1992) 255.

[37] T. Kyomen, H. Tamura, M. Oguni, M. Itoh, K. Kitayama, J. Phys.: Condens. Matter 9 (1997) 1841.

[38] M. Sayagues, M. Vallet-Regi, J. Hutchinson, J. Gonzalez-calbet, J. Solid State Chem. 125 (1996) 133.

[39] G. Burns, F.H. Dacol, D.E. Rice, D.J. Buttrey, M.K. Crawford, Phys. Rev. B 42 (1990) 10777.

[40] G. Amow, P.S. Whitfield, I.J. Davidson, R.P. Hammond, C.N. Munnings, S.J. Skinner, Ceram. Inter. 30 (2004) 1635.

[41] Y. Furukawa, S. Wada, T. Kajitani, S. Hosoya, J. Phys. Soc. Jpn. 68 (1999) 346.

[42] U.V. Lehmann, H. Muller-Buschbaum, Z. Anorg. Alleg. Chem. 470 (1980) 59.

[43] H. Takahashi, F. Munakata, M. Yamanaka, Phys. Rev. B 53 (1996) 3731.

[44] S.H. Byeon, G. Demaeau, Bull. Korean Chem. Soc. 15 (1994) 949.

[45] K. Asai, A. Yoneda, O. Yokokura, J.M. Tranquada, G. Shirane, J. Phys. Soc. Jpn. 67 (1998) 290.